

Temperature dependence of multi-jump magnetic switching process in epitaxial Fe/MgO (001) films*

Hu Bo(胡泊), He Wei(何为), Ye Jun(叶军), Tang Jin(汤进), Zhang Yong-Sheng(张永圣), Syed Sheraz Ahmad, Zhang Xiang-Qun(张向群), and Cheng Zhao-Hua(成昭华)[†]

State Key Laboratory of Magnetism and Beijing National Laboratory for Condensed Matter Physics, Institute of Physics, Chinese Academy of Sciences, Beijing 100190, China

(Received 19 March 2015; revised manuscript received 14 April 2015; published online 29 May 2015)

Temperature dependence of magnetic switching processes with multiple jumps in Fe/MgO (001) films is investigated by magnetoresistance measurements. When the temperature decreases from 300 K to 80 K, the measured three-jump hysteresis loops turn into two-jump loops. The temperature dependence of the fourfold in-plane magnetic anisotropy constant K_1 , domain wall pinning energy, and an additional uniaxial magnetic anisotropy constant K_U are responsible for this transformation. The strengths of K_1 and domain wall pinning energy increase with decreasing temperature, but K_U remains unchanged. Moreover, magnetization reversal mechanisms, with either two successive or two separate 90° domain wall propagation, are introduced to explain the multi-jump magnetic switching process in epitaxial Fe/MgO(001) films at different temperatures.

Keywords: multi-jump magnetic switching process, magnetoresistance, domain wall

PACS: 75.30.Gw, 75.60.Jk, 75.60.Ch

DOI: 10.1088/1674-1056/24/7/077502

1. Introduction

The magnetization reversal process is crucial when using Fe films for spintronic applications.^[1,2] Although Fe(001) film usually exhibits an intrinsic in-plane fourfold magnetic anisotropy, an additional uniaxial magnetic anisotropy (UMA)^[3,4] is always superimposed owing to the surface steps of substrates,^[5] oblique deposition,^[6] or dangling bonds.^[7] Depending on the strengths of the fourfold magnetic anisotropy constant K_1 , UMA constant K_U , and domain wall pinning energy, hysteresis loops will present one-, two-, and three-jump magnetic switching processes. When $K_U/K_1 < 1$, two-jump loops are observed.^[8,10] If the value of K_U is larger than 90°, with domain wall pinning energy at the same time, three-jump loops will be present at some directions of applied field. These magnetic switching processes can be understood by 90° domain wall nucleation. It is especially interesting that the one-jump process is also explained by two successive 90° domain wall nucleations instead of 180° domain wall nucleation, as was investigated by Zhan *et al.*^[11,12] But the temperature dependence of magnetic hysteresis loops with multiple jumps has been investigated little, even though it is important for the performance of magnetic media, random access memory, and the dynamic response of films. In our work, the pronounced UMA induced by oblique-incidence growth results in three-jump hysteresis loops in some directions of field in Fe/MgO (001) system. Moreover, these three-jump loops can transform into two-jump loops with decreasing temperature.

The K_1 , K_U , and domain wall pinning energy are researched by magnetoresistance (MR) measurements^[13,14] at different temperatures to explain this transformation.

2. Experiment

The Fe/MgO (001) films were deposited by molecular-beam epitaxy (MBE) in an ultrahigh vacuum (UHV) system with a base pressure of 2.0×10^{-10} mbar. The MgO (001) substrates were first heat treated at 700 °C for 2 h to obtain clean surfaces. The 30 monolayer (ML) Fe films with a deposition rate of 1.5 ML/min were grown by oblique-incidence deposition at room temperature. The incident Fe beam was at an angle of 10° with respect to the surface normal and with azimuthal angle along Fe [100] direction. Moreover, 25 ML Cu films were deposited as protective layers. The magneto-optical Kerr effect (MOKE) and MR measurements were used to research magnetic properties of film. The stable temperature is obtained using the LakeShore 340 temperature controller (stability < 0.01 °C/h) in the measurement. The MR measurements were performed with a standard four-point method at different temperatures, and the details are described in Ref. [14].

3. Results and discussion

The schematic configuration of the magnetic anisotropy and the coordinate system are shown in Fig. 1(a), which is used

*Project supported by the National Basic Research Program of China (Grant Nos. 2015CB921403, 2011CB921801, and 2012CB933102) and the National Natural Science Foundation of China (Grant Nos. 51427801, 11374350, and 11274361).

[†]Corresponding author. E-mail: zhcheng@aphy.iphy.ac.cn

in our MOKE measurement and data analysis. Based on the orientation of the additional in-plane UMA, the UMA along the hard axis of cubic magnetic anisotropy is defined as K_{U1} , which will be investigated in our other work of Fe (001) film grown at normal incidence geometry. Another UMA along Fe [100] originating from oblique-incidence growth geometry is defined as K_{U2} . It is perpendicular to the incident flux direction and results from the self-shadowing effect. The different directions of UMA can result in different magnetic switching processes. The UMA along Fe $[1\bar{1}0]$ hard axis makes the easy axis of cubic anisotropy inequivalent and has a small deviation from $\langle 100 \rangle$. The value of the deviation angle is given approximately by^[15]

$$\delta = \frac{1}{2} \sin^{-1} \left(\frac{K_{U1}}{K_1} \right).$$

The UMA along Fe [100] is important to create a multi-jump magnetic switching process. Zhan's experimental results reveal that one considerable UMA along [100] can result in three-jump loops at some directions of external magnetic field.^[11,16] These multi-jump loops were also observed in our sample with two considerable UMA in our work as illustrated in Fig. 1(b) one jump at $\theta_H = 9^\circ$, two jumps at $\theta_H = 135^\circ$, and three jumps at $\theta_H = 162^\circ$ given by typical MOKE; θ_H is the angle of applied field from [110] hard axis. According to the 90° domain wall magnetization reversal mechanism,^[16] magnetization from [100] to $[\bar{1}00]$ corresponds to the one-jump loops, from $[0\bar{1}0]$ to $[\bar{1}00]$ to $[010]$ corresponds to the two-jump loops, and from $[0\bar{1}0]$ to $[\bar{1}00]$ to $[100]$ to $[010]$ corresponds to the three-jump loops.

Compared with MOKE measurement, MR measurement has many advantages, such as high sensitivity in magnetic anisotropy energy,^[14] and no surface smoothness requirements.^[13] So the MR measurement equipped with temperature controller is a good method to investigate the temperature dependence of multi-jump magnetic switching process. In our previous work, the orientation of current is not strictly along [110] and has deviation as shown in inset of Fig. 2(a), which can distinguish the magnetization along the two easy axes. So the multi-jump switching process can also be revealed in MR measurement. For the Fe film, one-jump, two-jump or three-jump loops are observed respectively at different angles of applied field, as illustrated in Fig. 2 [one-jump at $\theta_H = 9^\circ$ (Fig. 2(a)), two-jump at $\theta_H = 135^\circ$ (Fig. 2(b)), and three-jump at $\theta_H = 162^\circ$ (Fig. 2(c))], which correspond to typical longitudinal MOKE measurements. We define the switching fields for the one-jump (H_C), for the two-jump (we refer to the first switching field as H_{C1} and to the second switching field as H_{C2}) and for the three-jump (we refer to the first switching field as H_{C1} , to the second switching field as H_C , and to the last switching field as H_{C3} , respectively) loops as shown in Fig. 2.

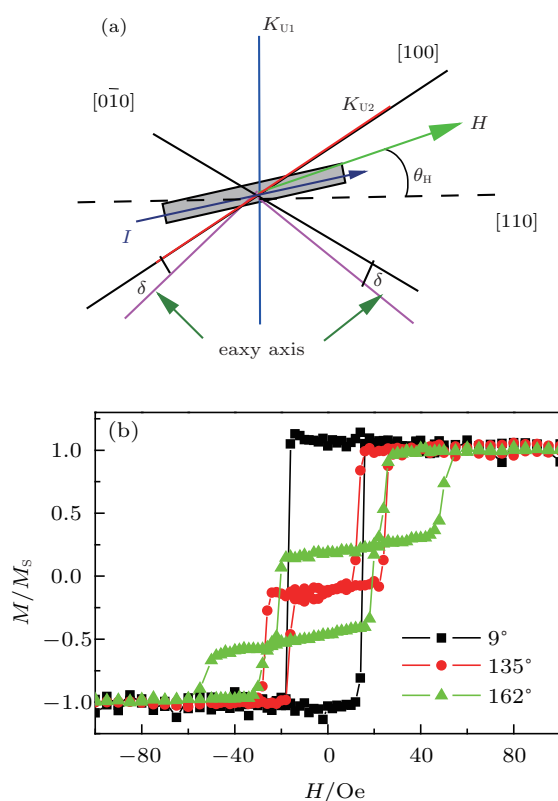


Fig. 1. (color online) (a) Definition of the orientation of in-plane fourfold anisotropy, two additional UMA K_{U1} , K_{U2} , and external magnetic field H used in film. (b) Typical longitudinal MOKE loops for film, with one-jump at $\theta_H = 9^\circ$, two-jump at $\theta_H = 135^\circ$, and three-jump at $\theta_H = 162^\circ$.

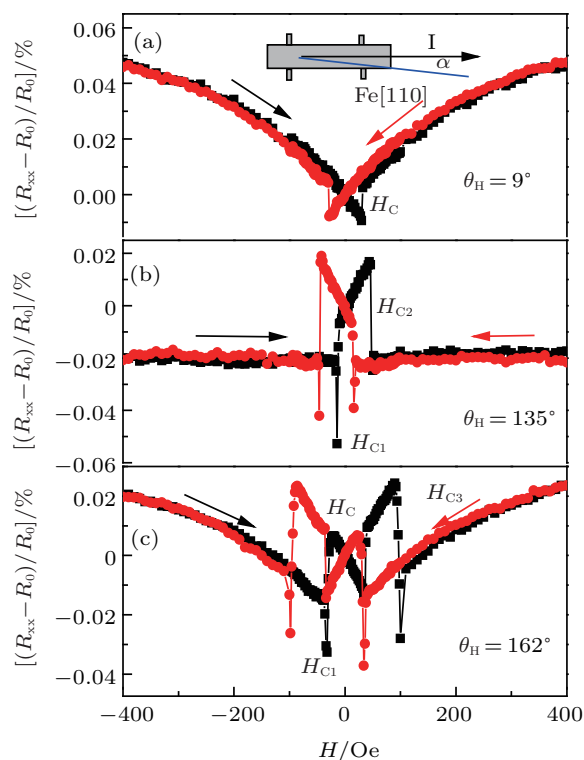


Fig. 2. (color online) Typical MR loops for film with (a) one-jump at $\theta_H = 9^\circ$, (b) two-jump at $\theta_H = 135^\circ$, and (c) three-jump at $\theta_H = 162^\circ$ corresponding to typical longitudinal MOKE measurements of Fig. 1. The orientation of current relative to the [110] is indicated in the inset of panel (a). The black (red) curves are for external magnetic field varying from negative (positive) to positive (negative) saturation.

The MR loops at $\theta_H = 108^\circ$ are measured at different temperatures (300 K–80 K) as shown in Fig. 3. Three-jump switching process is observed at 300 K. But the magnetic hysteresis loops turn into two-jump loops when the temperature decreases. This transformation can be well understood in terms of a competition of the cubic anisotropy K_1 , the extra UMA (K_{U1} , K_{U2}), and domain wall pinning energy.^[11,12,16]

In order to figure out K_1 , K_{U1} , and K_{U2} , the angular dependence of anisotropy magnetoresistances at high field of 400 Oe were measured at different temperatures, as shown in Fig. 4(a). The MR can be expressed as:^[14,17–20]

$$R_{XX} = R_{\perp} + (R_{//} - R_{\perp}) \cos^2(\theta_M - \alpha). \quad (1)$$

Here, θ_M and $\alpha = 6.3^\circ$ are angles of magnetic moment M and current, measured from the Fe[110] direction. The maximum value $R_{//}$ and minimum value R_{\perp} correspond to MR when H is parallel and perpendicular to the direction of current, respectively. The values of MR show a periodically oscillating behavior following the orientation of the external field. However, due to the magnetic anisotropy, M is no longer kept along with the external field H during rotation, i.e. the angular-dependent MR curves do not follow the $\cos^2(\theta_H - \alpha)$ relationship. The values of θ_M can be obtained by analyzing the MR curves on the basis of Eq. (1). Moreover, the magnetic torque can be expressed as $L(\theta_M) = \mu_0 M_S H \sin(\theta_H - \theta_M)$, and the normalized magnetic torque $l(\theta_M) = L(\theta_M) / \mu_0 M_S H = \sin(\theta_H - \theta_M)$

can be obtained at different temperatures, as illustrated in Fig. 4(b).

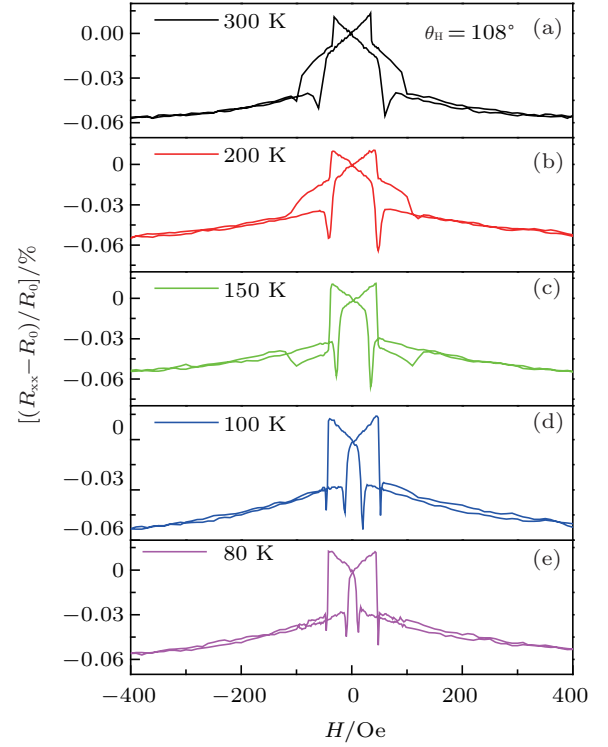


Fig. 3. (color online) MR loops for film of $\theta_H = 108^\circ$ at different temperatures: (a) 300 K, (b) 200 K, (c) 150 K, (d) 100 K, and (e) 80 K.

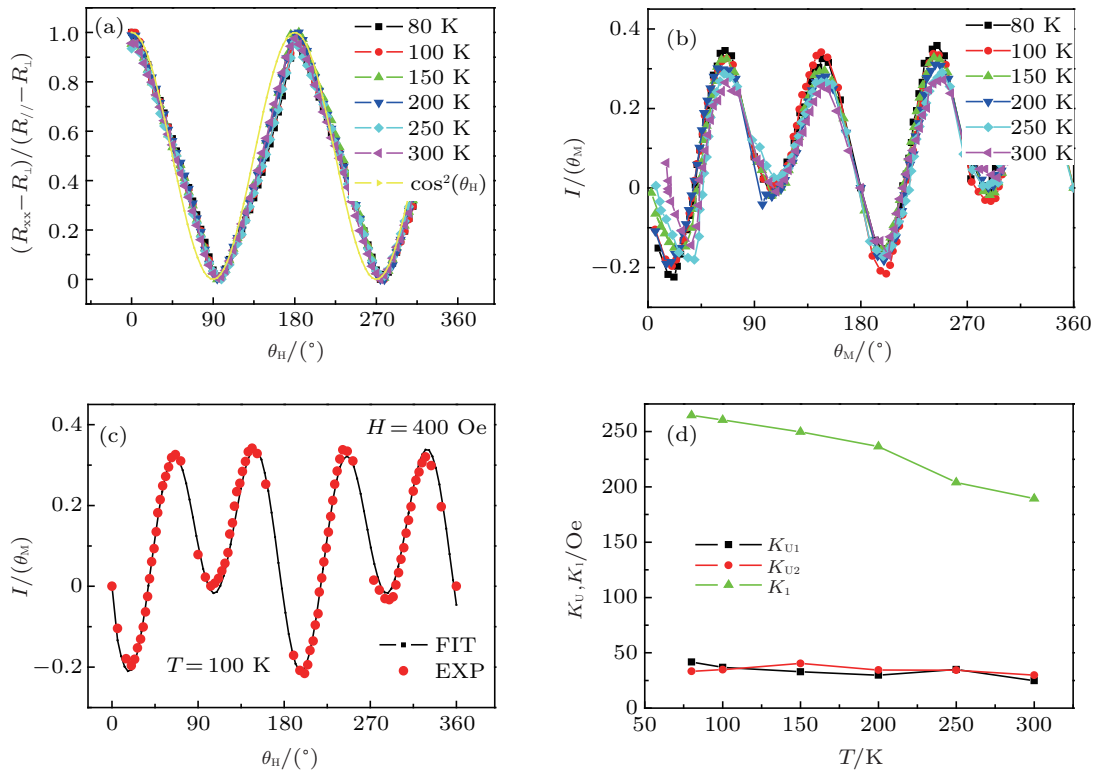


Fig. 4. (color online) (a) Angle-dependent MR measurement of $H = 400$ Oe at different temperatures and taking $\cos^2(\theta_H)$ as a reference for comparison and corresponding (b) magnetic torque (c) magnetic torque fitting curve of $H = 400$ Oe at 100 K. (d) The parameters of K_{U1} , K_{U2} , and K_1 , depending on temperature.

Considering the magnetic field is large enough to guarantee a single domain rotation in the Fe/MgO(001) system, the total energy including the magnetic anisotropy energy and Zeeman energy can be expressed as

$$E = K_{U1} \cos^2(\theta_M) + K_{U2} \sin^2\left(\theta_M - \frac{\pi}{4}\right) + \frac{K_1}{4} \cos^2(2\theta_M) - \mu_0 MH \cos(\theta_H - \theta_M). \quad (2)$$

In equilibrium state $\partial E / \partial \theta_M = 0$, the normalized magnetic torque is as follows:

$$l(\theta_M) = \frac{\left(-K_{U1} \sin(2\theta_M) + K_{U2} \cos(2\theta_M) - \frac{K_1}{2} \sin(4\theta_M)\right)}{\mu_0 MH}. \quad (3)$$

It can be easily seen that the $l(\theta_M)$ shows superposition of two UMA and fourfold magnetic anisotropies, as shown Fig. 4(c). Taking an example of the curve measured at $T = 100$ K, magnetic torque curve is fitted using Eq. (3) to get the magnetic anisotropy constants K_1 , K_{U1} , and K_{U2} . These parameters at other temperatures can be obtained similarly as shown in Fig. 4(d). The results show K_1 decreases with increasing temperature, while K_{U1} and K_{U2} remain unchanged. The fourfold magnetic anisotropy originates from magnetocrystalline anisotropy, which is interactions of the spontaneous magnetization and lattice. The spontaneous magnetization decreases with increasing temperature, which makes the value of K_1 also decrease. Moreover, the UMA results from shape anisotropy in our experiment, so the value of it is less influenced by the temperature.

Already, the 90° domain wall displacement has been introduced to interpret the multi-jump magnetic switching process.^[16] The strength of the domain wall pinning energy can be determined by fitting the angular dependence of the switching fields.^[15] We measured the switching fields (H_C , H_{C1} , H_{C2} , and H_{C3}) as a function of the angle θ_H at 4.5° interval for the Fe layers at different temperatures, and obtained a behavior similar to the one presented in Fig. 5(a) for the temperature $T = 200$ K.

The domain wall pinning energy can be derived from the equations of theoretical switching fields^[21]

$$H_{C1} = \frac{\varepsilon_{90^\circ-2\delta} + K_{U2}(\cos^2 \delta - \sin^2 \delta)}{M(\sin(\theta + \delta - \pi/4) + \cos(\theta - \delta - \pi/4))}, \quad 90^\circ \leq \theta \leq 135^\circ, \quad (4)$$

$$H_{C2} = \frac{\varepsilon_{90^\circ+2\delta} - K_{U2}(\cos^2 \delta - \sin^2 \delta)}{M(\cos(\theta - \delta - \pi/4) - \sin(\theta + \delta - \pi/4))}, \quad 90^\circ \leq \theta \leq 135^\circ, \quad (5)$$

$$H_{C3} = \frac{\varepsilon_{90^\circ-2\delta} - K_{U2}(\cos^2 \delta - \sin^2 \delta)}{M(\sin(\theta + \delta - \pi/4) + \cos(\theta - \delta - \pi/4))}, \quad 90^\circ \leq \theta \leq 135^\circ. \quad (6)$$

Due to K_{U1} , the minima of total energy (Eq. (3)) are located at $45^\circ + \delta$, $135^\circ - \delta$, $225^\circ + \delta$, and $315^\circ - \delta$. Because the angle between two neighboring easy axes in the system is either $90^\circ - 2\delta$ or $90^\circ + 2\delta$, the magnetization transitions in the multi-jump process are mediated by sweeping of $90^\circ - 2\delta$ or $90^\circ + 2\delta$ domain walls corresponding to domain wall pinning energies $\varepsilon_{90^\circ-2\delta}$ and $\varepsilon_{90^\circ+2\delta}$.

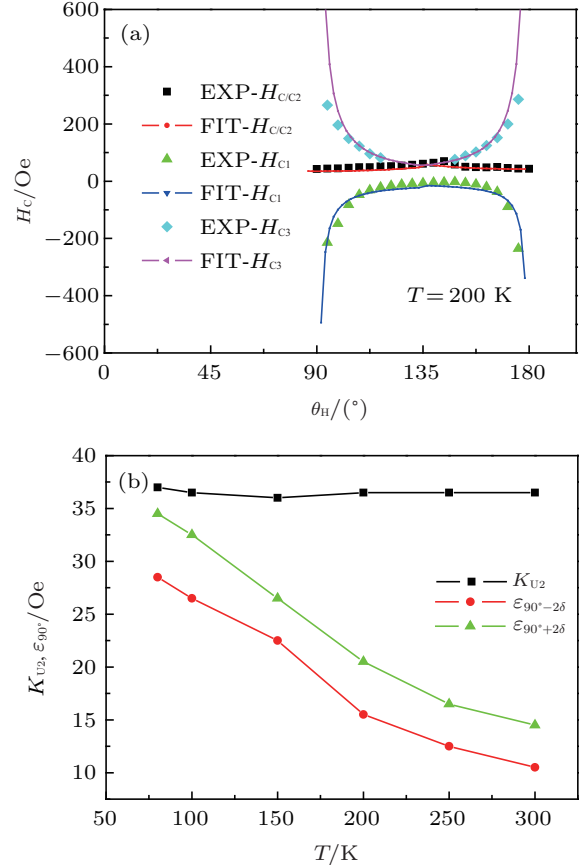


Fig. 5. (color online) (a) The experimentally observed switching fields H_{C2} , H_{C1} , and H_{C3} as functions of the field orientation, and the corresponding theoretical curves for these of sample at temperature 200 K. (b) The fitted parameters of K_{U2} , $\varepsilon_{90^\circ-2\delta}$, and $\varepsilon_{90^\circ+2\delta}$, depending on temperature.

The experimental results of switching fields H_C , H_{C1} , H_{C2} , and H_{C3} can be fitted well using the theoretical Eqs. (4)–(6), as illustrated in Fig. 5(a). On the basis of Zhan's results, the 180° magnetic transitions (H_C) can be understood by the fact that they consist of two successive 90° magnetic transitions; one is at H_{C2} and another 90° magnetic transition immediately follows at the same field H_{C2} .^[11,12] This indicates that the theoretical expression for H_{C2} , which corresponds to a 90° DW nucleation, allows us to nicely fit the H_C data. By fitting observed switching fields at different temperatures, the temperature dependence values of K_{U2} , $\varepsilon_{90^\circ-2\delta}$, and $\varepsilon_{90^\circ+2\delta}$ are obtained, as shown in Fig. 5(b). The results show that the UMA constant K_{U2} is independent of temperature and keeps constant, which is consistent with the MR results. But the values of domain wall pinning energies $\varepsilon_{90^\circ-2\delta}$ and $\varepsilon_{90^\circ+2\delta}$ both

decrease largely from 35 Oe to 10 Oe and 30 Oe to 8 Oe, respectively, when the temperature increases from 80 K to 300 K.

By analyzing the angle θ_H of Fe layers with one-, two-, and three-jump loops at different temperatures, the range of these multi-jump loops varies, as illustrated in Fig. 6(a). The number represents the type of switching process. When the temperature increases, the range of loops with one jump keeps constant. The two-jump loops turn into three-jump loops, and their range becomes narrow. So the loops with two and three jumps are greatly dependent upon temperature. In order to research this transformation, the 90° domain-wall pinning energies and total energy of Fe (001) system obtained in previous analysis were introduced.

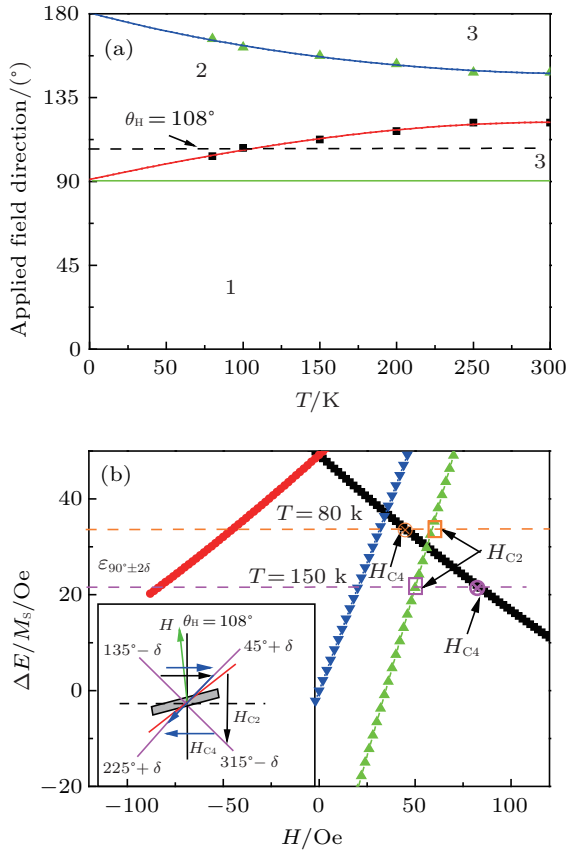


Fig. 6. (color online) (a) The applied field directions of one-, two-, and three-jump loops, varying with temperature. The dashed line indicates the direction of the applied field at $\theta_H = 108^\circ$ (b) Energy differences $\Delta E_{135^\circ - \delta \rightarrow 45^\circ + \delta}$ (blue), $\Delta E_{315^\circ - \delta \rightarrow 225^\circ + \delta}$ (black), $\Delta E_{225^\circ + \delta \rightarrow 315^\circ - \delta}$ (red), and $\Delta E_{45^\circ + \delta \rightarrow 315^\circ - \delta}$ (green) as a function of the applied field for sample at $\theta_H = 108^\circ$. The inset is schematic diagram of the two- and three-jump magnetization switching process.

Based on the obtained values of K_{U1} , K_{U2} , K_1 , and total energy Eq. (2), figure 6(b) shows in the energy differences $\Delta E_{135^\circ - \delta \rightarrow 45^\circ + \delta}$ (blue), $\Delta E_{315^\circ - \delta \rightarrow 225^\circ + \delta}$ (black), $\Delta E_{225^\circ + \delta \rightarrow 315^\circ - \delta}$ (red), and $\Delta E_{45^\circ + \delta \rightarrow 315^\circ - \delta}$ (green) as a function of the applied field in direction $\theta_H = 108^\circ$ (dashed lines in Fig. 6(a)). On the basis of Ref. [16], the two-jump

switching process at $\theta_H = 108^\circ$ corresponds to magnetization switching from $135^\circ - \delta$ to $45^\circ + \delta$ and $45^\circ + \delta$ to $315^\circ - \delta$ by two separate 90° domain wall nucleations as shown in inset of Fig. 6(b) (black arrow). But in three-jump switching process ($135^\circ - \delta$ to $45^\circ + \delta$ to $225^\circ + \delta$ to $315^\circ - \delta$ blue arrow), the magnetization switching between $45^\circ + \delta$ and $225^\circ + \delta$ should overcome two energy barriers ($45^\circ + \delta \rightarrow 315^\circ - \delta$) and ($315^\circ - \delta \rightarrow 225^\circ + \delta$) by means of two successive 90° domain wall nucleations. So we plot the energy differences between these directions as a function of the applied field.

Corresponding to two different 90° domain wall nucleation processes, we focus on the two energy barriers ($45^\circ + \delta \rightarrow 315^\circ - \delta$) and ($315^\circ - \delta \rightarrow 225^\circ + \delta$) that guide the magnetization switching process. The switching field H_{C2} is determined by the energy barrier for the transition $\Delta E_{45^\circ + \delta \rightarrow 315^\circ - \delta} = \epsilon_{90^\circ + 2\delta}$. The other energy barrier $\Delta E_{315^\circ - \delta \rightarrow 225^\circ + \delta}$ decreases with increasing applied field and becomes $\epsilon_{90^\circ - 2\delta}$ (which is close to $\epsilon_{90^\circ + 2\delta}$) at H_{C4} (as shown in Fig. 6(b)). Based on the results of Ref. [16], when $H_{C4} > H_{C2}$, the domains along $315^\circ - \delta$ are unstable and cannot grow; the magnetization switching is from $45^\circ + \delta$ to $225^\circ + \delta$ directly. So, the magnetic loops will present a three-jump loop ($135^\circ - \delta$ to $45^\circ + \delta$ to $225^\circ + \delta$ to $315^\circ - \delta$) by two successive domain wall nucleations. Otherwise, when $H_{C2} > H_{C4}$, the domains along $315^\circ - \delta$ are stable and can grow; the magnetization switching is from $45^\circ + \delta$ to $315^\circ - \delta$ and magnetic loops present two-jump loops ($135^\circ - \delta$ to $45^\circ + \delta$ to $315^\circ - \delta$) by two separate 90° domain wall nucleations. Taking $T = 80$ K and 150 K for example, the values of $\epsilon_{90^\circ - 2\delta}$ and $\epsilon_{90^\circ + 2\delta}$ decrease with increasing temperature, which makes the relationship $H_{C2} > H_{C4}$ turn into $H_{C2} < H_{C4}$. So the transformation of two-jump loop into three-jump loop appears.

4. Conclusion

Fe/MgO (001) films with one-, two-, and three-jump magnetic switching processes were fabricated. The magnetic hysteresis loops with two-jump change into three-jump loops with increasing temperature. This can be explained by temperature dependence of magnetic anisotropy energy and domain wall pinning energy. The fourfold in-plane magnetic anisotropy energy (K_1), two additional UMA energy (K_{U1}, K_{U2}), and domain-wall pinning energies were obtained by MR measurements. As the temperature decreases, the values of K_1 and domain wall pinning energies increase, but K_{U1} and K_{U2} remain largely unchanged. These temperature dependencies of parameters make the reversal mechanism from two successive 90° domain-wall propagations turn into two separate domain-wall propagations.

References

- [1] Johnson M T, Bloemen P J H, Den Broeder F J A and Vries J J D 1996 *Rep. Prog. Phys.* **59** 1409
- [2] Gould C, Pappert K, Schmidt G and Molenkamp L W 2007 *Adv. Mater.* **19** 323
- [3] Gould C, Rüster C, Jungwirth T, Girgis E, Schott G M, Giraud R, Brunner K, Schmidt G and Molenkamp L W 2004 *Phys. Rev. Lett.* **93** 117203
- [4] Tian C S, Qian D, Wu D, He R H, Wu Y Z, Tang W X, Yin L F, Shi Y S, Dong G S, Jin X F, Jiang X M, Liu F Q, Qian H J, Sun K, Wang L M, Rossi G, Qiu Z Q and Shi J 2005 *Phys. Rev. Lett.* **94** 137210
- [5] Wu Y Z, Won C and Qiu Z Q 2002 *Phys. Rev. B* **65** 184419
- [6] Cherifi S, Hertel R, Locatelli A, Watanabe Y, Potdevin G, Ballestrazzi A, Balboni M and Heun S 2007 *Appl. Phys. Lett.* **91** 092502
- [7] Zhao H B, Talbayev D, Lüpke G, Hanbicki A T, Li C H, van't Erve M J, Kioseoglou G and Jonker B T 2005 *Phys. Rev. Lett.* **95** 137202
- [8] Fan Y, Zhao H B, Lüpke G, Hanbicki A T, Li C H and Jonker B T 2012 *Phys. Rev. B* **85** 165311
- [9] Jeong Y, Lee H, Lee S, Yoo T, Lee S, Liu X and Furdyna J K 2014 *Solid State Commun.* **200** 1
- [10] Caminale M, Moroni R, Torelli P, Lin W C, Canepa M, Mattera L and Bisio F 2014 *Phys. Rev. Lett.* **112** 037201
- [11] Zhan Q F, Vandezande S, Haesendonck C V and Temst K 2007 *Appl. Phys. Lett.* **91** 122510
- [12] Zhan Q F, Vandezande S, Temst K and Haesendonck C V 2009 *New J. Phys.* **11** 063003
- [13] Tripathy D, Vavassori P, Porro J M, Adeyeye A O and Singh N 2010 *Appl. Phys. Lett.* **97** 042512
- [14] Ye J, He W, Wu Q, Liu H L, Zhang X Q, Chen Z Y and Cheng Z H 2013 *Sci. Rep.* **3** 2148
- [15] Daboo C, Hicken R J, Gu E, Gester M, Gray S J, Eley D E P, Ahmad E, Bland J A C, Ploessl R and Chapman J N 1995 *Phys. Rev. B* **51** 15964
- [16] Zhan Q F, Vandezande S, Temst K and Haesendonck C V 2009 *Phys. Rev. B* **80** 094416
- [17] Krivorotov I N, Leighton C, Nogués J, Schuller Ivan K and Dan Dahlberg E 2002 *Phys. Rev. B* **65** 100402
- [18] Cao W N, Li J, Chen G, Zhu J, Hu C R and Wu Y Z 2011 *Appl. Phys. Lett.* **98** 262506
- [19] Li J, Jin E, Son H, Tan A, Cao W N, Hwang C and Qiu Z Q 2012 *Rev. Sci. Instrum.* **83** 033906
- [20] Gruyters M 2006 *Phys. Rev. B* **73** 014404
- [21] Cowburn R P, Gray S J, Ferré J, Bland J A C and Miltat J 1995 *J. Appl. Phys.* **78** 7210